Energy Conversion and Management 150 (2017) 651–668

Contents lists available at ScienceDirect

Energy Conversion and Management

journal homepage: www.elsevier.com/locate/enconman

Performance analysis of different working gases for concentrated solar gas engines: Stirling & Brayton

Mohamed A. Sharaf Eldean[a,*], Khwaja M. Rafi[b], A.M. Soliman[a,c]

[a] Department of Engineering Science, Faculty of Petroleum & Mining Engineering, Suez University, Suez 43722, Egypt
[b] JahangirAbad Institute of Technology, Jahangir Abad, India
[c] Mechanical Engineering Department, Faculty of Engineering, Al Jouf University, Sakaka, Saudi Arabia

ARTICLE INFO

Keywords:
Concentrated solar dish
Stirling cycle
Brayton cycle
Modeling & simulation
Working gases

ABSTRACT

This article presents a performance study of using different working fluids (gases) to power on Concentrated Solar Gas Engine (CSGE-Stirling and/or Brayton). Different working gases such as Monatomic (five types), Diatomic (three types) and Polyatomic (four types) are used in this investigation. The survey purported to increase the solar gas engine efficiency hence; decreasing the price of the output power. The effect of using different working gases is noticed on the engine volume, dish area, total plant area, efficiency, compression and pressure ratios thence; the Total Plant Cost (TPC, $). The results reveal that the top cycle temperature effect is reflected on the cycle by increasing the total plant efficiency (2–10%) for Brayton operational case and 5–25% for Stirling operational case. Moreover; Brayton engine resulted higher design limits against the Stirling related to total plant area, m^2 and TPC, $ while generating 1–100 MW_e as an economic case study plant. C_2H_2 achieved remarkable results however, CO_2 is considered for both cycles operation putting in consideration the gas flammability and safety issues.

1. Introduction

The harmony between environmental protection and economic growth has become a worldwide concern, there is an urgent need to effectively reuse solar energy. Such a source of clean energy is one of the most attractive renewable energy that can be used as for heat engines [1]. The solar radiation can be focused onto the displacer hot-end of the gas engine, thereby creating a solar powered prime mover [2]. Concentrated Solar Gas Engine (CSGE) is one of the oldest solar technologies. There are a wide number of past projects, mostly in Europe, Japan, Australia and in USA related to the concentrated solar Stirling engine (CSSE). The most widely used engines for such technology is the solar Stirling engine [3–7]. CSSE has some advantages concluded into:

- Such systems have medium concentration ratio (500–1000).
- The systems are modular, each system is a self-contained power generator, they can be assembled into plants ranging in size from a kilo-watts to 100 MW [3].
- CSSE is simple in design and construction and continuous tracking with the sun.

The main working fluids of these engines are the gases. Hydrogen, Air, Helium, and Nitrogen are usually applied to get the required power from Stirling engines. High temperature and pressure Stirling engines such as KocKums, STM, and SOLO-161 are the real examples for the use of Hydrogen and Helium [2]. Hossien [8] reported the performance of the solar powered Stirling engine for electricity by the use of Hydrogen as a working gas. Koichi Hirata [9] investigated a compact and low-cost Stirling engine operated with Helium, Air, and Nitrogen. Ihsan [10] examined a V-type Stirling engine having two heaters with Helium working gas, which the maximum power not exceeded over 118 W. Cinar [11] investigated Helium working gas with gamma Stirling engine for 1 kW and 1000 °C. Wu et al. [12] studied the optimal performance of a Stirling engine where the results showed that Stirling engine cycle was different in efficiencies according to the use of different characters of the working fluids (Air and Helium). Rix [13] studied the effect of air operation on the 0.5 kW Stirling engine. Currently, the contending Stirling engines for dish/engine systems include the SOLO-161 (11-kW), the KocKums (25-kW) and the Stirling Thermal-Motors STM 4–120 (25-kW) are using not more than two working gases (Air, Helium) [14]. It is obvious from literatures that the power produced from the Stirling engine didn't exceed over 25–50 kW where the power enhancement procedures are still under investigations. Moreover; Brayton cycle or Otto cycle is yet under investigation of operation with

* Corresponding author.
E-mail addresses: mohammed.eldeen@suezuniv.edu.eg (M.A. Sharaf Eldean), kmrafi1@gmail.com (K.M. Rafi), ahsoliman69@hotmail.com (A.M. Soliman).

http://dx.doi.org/10.1016/j.enconman.2017.08.008
Received 18 May 2017; Received in revised form 3 August 2017; Accepted 4 August 2017

Nomenclature

A	cross-sectional area, m^2
A_{dish}	dish area, m^2
A_p	piston area, m^2
C_p	specific heat capacity, kJ/kg °C @ constant pressure
C_v	specific heat capacity, kJ/kg °C @ constant volume
CSBE	concentrated solar Brayton engine
CSSE	concentrated solar Stirling engine
CR	compression ratio, concentration ratio for the dish
D	diameter, m
f	focal length, m
H_{dish}	dish parabola height, m
I_s	solar intensity, W/m^2
MEP	mean effective pressure, bar
m	mass flow rate, kg/s
NOD	number of dishes
NOC	number of cylinders
P	pressure, bar
P_{BE}	Brayton engine power, kW
P_{SE}	Stirling engine power, kW
P_{total}	total power, kW
R	specific gas constant, kJ/kg °C
RA	rim angle, °
RAR	rim angle ratio
r.p.m	speed, rev/min
r_p	pressure ratio
T	temperature, °C
TPC	total plant costs, $
V	volume, cm^3
v	specific volume, m^3/kg
W	work, kW

Subscripts

a	actual
atm	atmospheric
BE	Brayton engine
comp	compressor
EG	electric generator
g	gas
h	high
i	inlet
l	low
opt	optical
o	out
p	piston
SE	stirling engine
t	turbine, tube

Greek

η	efficiency
γ	isentropic index
ϕ	correction factor for Brayton efficiency

concentrated solar dish [15]. Brayton gas plants are applied exclusively for solar chimney or concentrated solar towers powered by air or helium working gases [16]. Generally, the CSSE power is considered low compared with the dish area (almost 100 m^2 for 25 kW). Add to this, there is a high production cost of CSSE with limited endurance and heavy weight [9]. The novelty of this work is to investigate and compare different concentrated solar gas engines (CSGE Brayton and Stirling) related to different working gases instead of conventional gases (Air and Helium). The work is trying to emphasize the gained power from the gas engine by examining more working gases. This study is not investigated before related to the diversities of the working gases that being used. The primary aim of investigating these working gases (Monatomic-5types, Diatomic-3types, and Polyatomic-4types) is to enhance the system execution by scaling down the dish area and increasing the total plant efficiency. The comparison is constructed in order to optimize the power produced from CSGE by seeking high efficiency thence; lowering the production price. The study is established according to the following items:

- New working gases are compared related to the terms of compression ratio, pressure ratio, efficiency and design limits (dish area, receiver area, focal distance, power, and so on).
- Monatomic gases (He, Ar, Ne, Kr, Xe), Diatomic gases (Air, H_2, N_2), and Polyatomic gases (CO_2, NH_3, CH_4, C_2H_2) are investigated in this study.
- The working gas election is performed according to best compression and pressure ratios results.
- Stirling and Brayton engines are compared related Total Plant Cost (TPC, $) and design limits of the plant.
- Wide scope of operating conditions (400–900 °C) and total plant power (1–100 MWe) are investigated and compared.
- REDS-SDS [17,18] is used as a powerful tool box for modeling and simulation of the proposed solar engines.

2. Concentrated solar gas engines: modeling & simulation

2.1. Modeling toolbox

The proposed system is modeled by the aid of REDS-SDS software which is developed by Sharaf et al. [17,18]. The model configuration contains the following; Parabolic Dish Concentrator (PDC), and gas engine for power generation. The model scheme has the ability to be operated by Stirling or Brayton engines which the designer receives the ability to select between these two engines. Moreover; the ability to select between 12 different working gases is also allowable. Rim angle degree values are stored in the submenu of the model and the user can easily select between the range of 15° up to 150°. Optical performance values are stored in the sub-menu of performance. The unknown parameters are the areas, dimensions, mass flow rates, engine volume, and the process temperatures are calculated. In this work, the power production is specified as a known parameter in order to calculate the design limits. The total electrical load would calculate the total plant dishes and other design specifications. Fig. 1 shows the CSGE model program.

2.2. The calculation methodology & assumptions

The developed model is built based on **design** technique aspects of modeling not **performance** technique [17,18]. In performance model, areas flow rates and design limits are assigned (existing system) in order to calculate and measure the power, top cycle temperature, efficiency and performance (The efficiency). However; in the design model (current case study), the power, top cycle temperature, and efficiencies are assigned and known in order to calculate and measure the design limits such as, areas, diameters, flow rates, required costs, etc. For example, the top and bottoming temperatures ranges are specified as 400–900 °C for the top range and 25 °C for the bottom.

For solar radiation and due to the low thermal inertia, a dish Stirling System reacts very quickly on changes in solar thermal input. Thus,

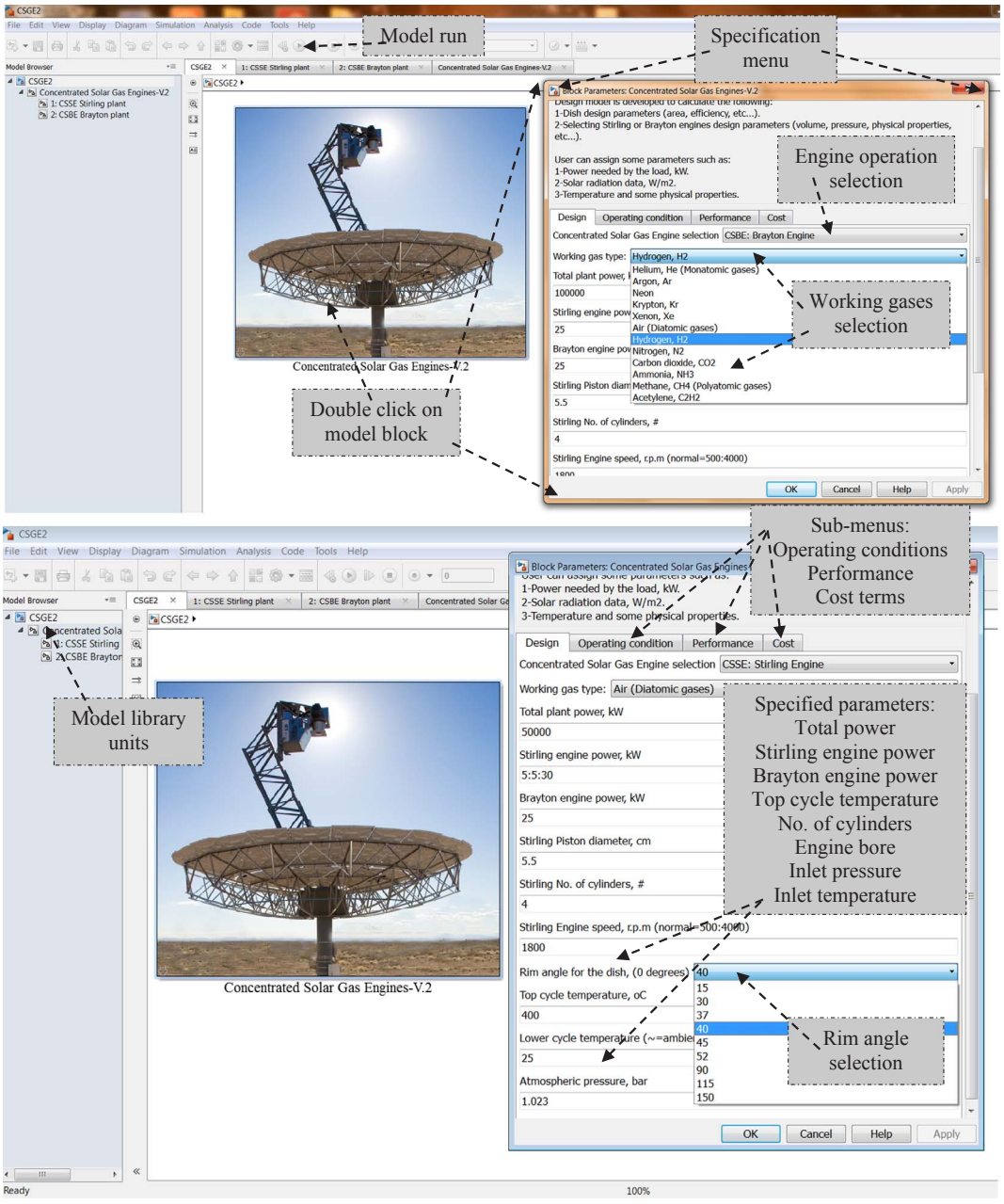

Fig. 1. Model diagram of REDS-SDS tool box for the CSGE plant [17,18].

steady state operation is achieved within a few minutes after system start. A typical daily pattern of net electric energy production over a day is given in Fig. 2 below. From the diagram, it can be seen that a dish Stirling system already starts net electric energy production when direct beam insolation (DNI) reaches values around 200–300 W/m^2 (DNI) in the morning, depending on mechanical and thermal losses of the engine as well as the optical performance of the concentrator.

Maximum power output is normally reached at 1000 W/m^2 or (DNI). For solar radiation, 1000 W/m^2 is assumed for this study in order to fix the dish area (lowering the initial costs), and maximizing the power output while measuring the compression and pressure ratios. An insolation of 1000 W/m^2 is known as the "Full Sun" [29]. Table 1 shows the specified and calculated terms of the proposed model based on the design technique of modeling.

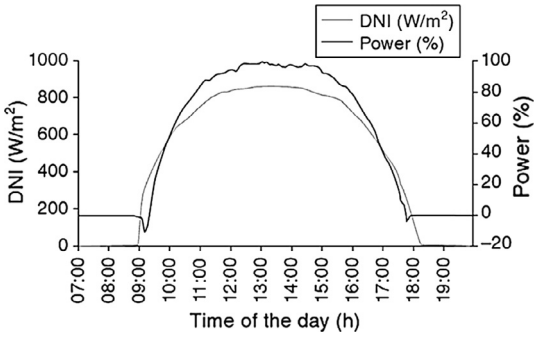

Fig. 2. Daily power output of a grid connected dish Stirling system with favorable irradiation [29].

Table 1
The specified parameters based on the concept of design technique of modeling.

Specified	Calculated
(1) Design limits	
Total plant power, kW = 1000–100,000	Dish concentration ratio
Stirling engine power, kW = 5–30	Dish area, m^2
Stirling engine No. of cylinders = 4	Receiver area, m^2
Stirling engine piston bore, cm = 5.5–6 [19]	Total plant area, m^2
Stirling engine speed, r.p.m = 1000–3500	Dish parabola height, m
Brayton engine power, kW = 5–30	Rim angle ratio
Top cycle temperature, ˚C = 400–900	Focal length, m
Lower cycle temperature, ˚C = 25	No. of dishes
Lower cycle pressure, bar = 1.023	Compression ratio (Stirling & Brayton)
Rim angle = 39–40˚ [20]	Pressure ratio (Stirling & Brayton)
	Max and Min specific volumes, m^3/kg (Stirling & Brayton)
	Top cycle pressure, bar (Stirling & Brayton)
	Stirling piston volume/cylinder, cm^3 (Stirling)
	Stirling piston stroke, cm (Stirling)
	Mean effective pressure, bar (Stirling & Brayton)
	Gas turbine and compressor power, kW (Brayton cycle)
	Outlet compressor temperature, ˚C (Brayton)
	Gases mass flow rate, kg/s (Brayton)
	Turbine speed, r.p.m (Brayton)
Specified	
(2) Operating conditions	
Solar radiation, W/m^2 = 1000	
Ambient temperature, ˚C = 25	
Operating hours, h = 10	
Specified	Calculated
(3) Performance	
Generator efficiency, % = 95	Stirling engine efficiency, %
Receiver efficiency, % = 70–94 (depending to temperature)	Brayton engine efficiency, %
Dish mirror efficiency, % = Aluminum, acrylic, 98 [20]	Total plant efficiency, %
Absorptivity of the receiver, % = 94	
Specified	Calculated
(4) Cost [19]	
Dish cost, $\$/m^2$ = 300	Total plant cost, $ = Direct costs + 15% × Direct costs
Receiver cost, $\$/m^2$ = 185	
Engine cost, $/kW = 370–450	
Site costs, $\$/m^2$ = 2.2	
Indirect cost, % = 13–15 of direct cost	
Operating & Maintenance cost, $/kW year = 37	

2.3. The mathematical model

2.3.1. CSSE mathematical model

The solar powered gas engine system uses a large parabolic a mirror to focus the sun rays on the hot side of a gas engine. The reflective mirrors are mounted on a parabolic-shaped structure using stamped sheet metal. Other structure accessories are constructed of steel. The good solar dish reflectors must have the following properties; reasonable weight; hardness against deflection and wind load, durability against moisture and temperature changes; parts must be flexible; low cost, effective reflecting materials; and long lifetime [20]. The following equations are representing the dish calculation model. By assigning the total plant power and the engine power, the total number of the plant dishes is calculated.

$$NOD = \frac{P_{total}}{P_{SE}} \tag{1}$$

The actual Stirling engine efficiency is calculated from the following equation [2,21,22]:

$$\eta_{SE} = 0.5 \times \left(1 - \frac{T_l}{T_h}\right) \tag{2}$$

The Stirling engine volume ratio (compression ratio) based on the efficiency is obtained as follows [2]:

$$\tau = \frac{T_h}{T_l} \tag{3}$$

$$\Theta = \frac{\frac{1-\left(\frac{1}{\tau}\right)}{\eta_{SE}} - 1}{1-\left(\frac{1}{\tau}\right)} \tag{4}$$

$$CR_{SE} = e^{\left(\frac{C_v}{R \times \Theta}\right)} \tag{5}$$

where C_v is the specific heat capacity of the gas at constant volume, kJ/kg ˚C, and R is the specific gas constant, kJ/kg ˚C. The Stirling pressure ratio is then calculated by the calculating of the top cycle pressure:

$$P_h = P_l \times CR_{SE} \times \frac{T_h}{T_l} \tag{6}$$

The pressure ratio is then calculated:

$$r_{P_{SE}} = \frac{P_h}{P_l} \tag{7}$$

The total plant efficiency is obtained by the assigning generator efficiency and optical and receiver efficiencies:

$$\eta_{total} = \eta_{SE} \times \eta_{EG} \times \eta_{rec} \times \eta_{opt} \tag{8}$$

Dish mirror area, m^2:

$$A_{dish} = \frac{P_{SE}}{I_s \times \eta_{total}} \tag{9}$$

where I_s is the solar radiation, W/m^2. Rim angle ratio (RAR) is calculated from the following sequence [24]:

$$RAR = 1.003 \times e^{-\left(\frac{RA-11.28}{13.86}\right)^2} + 2.186 \times e^{-\left(\frac{RA+100.2}{127.6}\right)^2} \tag{10}$$

where RA is the rim angle in degree. The dish focal length f is calculated in m:

$$f = RAR \times D_{dish} \tag{11}$$

The dish parabola height, m [20]:

$$H_{dish} = \frac{D_{dish}^2}{16 \times f} \tag{11}$$

The calculations of the dish concentration ratio $CR = A_{dish}/A_{rec}$ [22–24] is obtained through the following sequence:

$$\Psi = \left(\frac{T_{amb}}{T_h}\right) \times \left(\frac{1}{5 \times T_h^4 - T_{amb}^4 + 4 \times T_h^3}\right) \tag{12}$$

$$CR_{dish} = \frac{\sigma = 5.669e^{-8}}{0.9 \times \alpha_{rec} \times Is \times \Psi)} \tag{13}$$

Then the receiver area, m^2 is calculated:

$$A_{rec} = \frac{A_{dish}}{CR_{dish}} \tag{14}$$

The total plant surface area, m^2:

$$A_{total} = A_{dish} \times NOD \tag{15}$$

The mean effective pressure is calculated as follows [2]:

$$MEP = \frac{P_{atm} \times (CR_{SE} + 1) \times (\tau + 1)}{4} \quad (16)$$

Therefore; the Stirling engine piston dimensions is calculated [2]: And the piston volume, cm^3:

$$V_p = \frac{60 \times P_{SE}}{4\pi \times NOC \times \times MEP \times r.\,p.\,m \times F \times \frac{T_h - T_l}{T_h + T_l}} \quad (17)$$

where *NOC* is the number of cylinders, and the *F* parameter is equal to 0.25–0.35 [2]. The stroke, cm:

$$Stroke = \frac{V_p}{A_p} \quad (18)$$

Fig. 3 shows a schematic diagram of the CSSE cycle and the T-S and P-V diagrams.

2.3.2. CSBE mathematical model

In a dish/Brayton system, solar heat is used to replace (or supplement) the fuel. The resulting hot gas expands rapidly and is used to produce power. In the gas turbine, the burning is continuous and the expanding gas is used to turn a turbine and alternator. As in the Stirling engine, recuperation of waste heat is a key to achieving high efficiency. Dish equations (areas, concentration ratio, focal length, etc.) from the previous subsection is not repeated here. The Brayton cycle ideal efficiency is performed as follows [21]:

$$\eta_{BE} = 1 - \sqrt{\frac{T_l}{T_h}} \quad (19)$$

The actual Brayton efficiency is calculated as following [27];

$$\eta_{BE_a} = \phi \times \eta_{BE} \quad (20)$$

where ϕ is a correlation factor that been obtained at the pressure ratio rage of 2–30 and temperature range of 300–1100 °C, turbine and compressor efficiencies are 85% and 75% respectively. Appendix B shows the calculations of the optimum Brayton efficiency based on cycle temperatures.

$$\phi = 0.1699 \times \epsilon^{0.001002 \times T_h} - 4.864e + 13 \times \in^{-0.1102 \times T_h} \quad (21)$$

The Brayton engine volume ratio (compression ratio-*CR*) based on the actual efficiency is then obtained as follows:

$$CR_{BE} = \left(\frac{1}{1 - \eta_{BE_a}}\right)^{\left(\frac{1}{\gamma - 1}\right)} \quad (22)$$

The Brayton pressure ratio is then calculated:

$$r_p = \left(\frac{1}{1 - \eta_{BE_a}}\right)^{\left(\frac{\gamma}{\gamma - 1}\right)} \quad (23)$$

The compressor power, kW:

$$W_{comp} = \frac{P_{BE}}{\eta_{BE_a} \times \eta_{EG}} \quad (24)$$

The turbine power, kW:

$$W_t = W_{comp} + P_{BE} \quad (25)$$

Outlet turbine temperature, °C:

$$Tto = \frac{T_h}{r_p^{\left(\frac{\gamma - 1}{\gamma}\right)}} \quad (26)$$

Brayton cycle mass flow rate, kg/s:

$$m_{\dot{g}} = \frac{Wt}{C_p \times (T_h - T_{to})} \quad (27)$$

Outlet compressor temperature, °C:

$$T_{comp_o} = \left(\frac{W_{comp}}{m_{\dot{g}} \times C_p}\right) + T_l \quad (28)$$

Fig. 4 shows a schematic diagram of the CSBE cycle and the T-S diagram.

2.3.3. The model validation

The proposed cycle is mathematically modeled where the design and performance calculations are performed using the developed program with the aid of MatLab/SimuLink toolbox [17,18]. The considered and selected working fluids in this work are examined and operated under different operating conditions. Under the same operating conditions, the obtained results are compared with the results of Abbas et al. [3]. The comparison shows a very good agreement between the two models as shown in Table 2. This indicates the validity of the results and the reliability of the development program for the CSGE. The error percentage (3.5%) is in acceptable range between the developed model and Abbas [3] which is caused by the using of different equations and different technique of modeling.

3. The proposed working gases

The hot gas Stirling and/or Brayton engines are considered as a simple type of engines that use a compressible fluid as the working fluid. Heat transfer to the working fluid is very important. High mass flow is needed for better heat transfer. Moreover; thermodynamic properties of the working gas of the gas engines have the biggest influence of possibility to achieve high energetic efficiency. Fast exchange of heat is the main factor of working gas selection. As it seen from literature that CSGE is mainly operated by not more than three gases (Air, Helium, and Hydrogen). Therefore; in this work, twelve working gases are examined for two types of engines (Stirling and Brayton).

3.1. Classifications & physical properties

The proposed working gases in this study are classified into main three categories according to their chemical structure:

- Monatomic gases (Helium-He, Argon-Ar, Neon-Ne, Krypton-Kr, Xenon-Xe).
- Diatomic gases (Air, Hydrogen-H_2, Nitrogen-N_2).
- Polyatomic gases (Carbon dioxide-CO_2, Ammonia-NH_3, Methane-CH_4, Acetylene-C_2H_2).

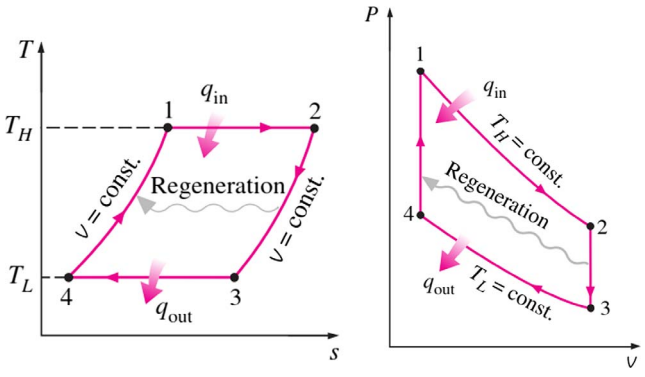

Fig. 3. Schematic diagram of CSSE cycle and the T-S diagram [28].

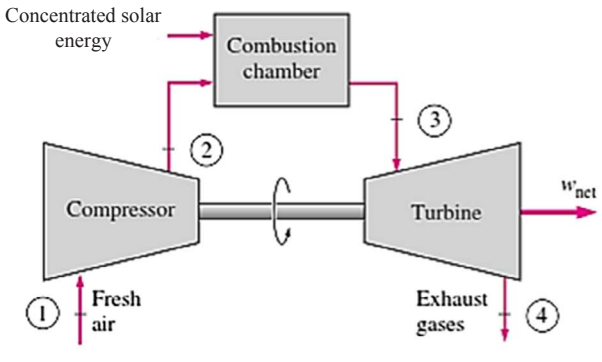

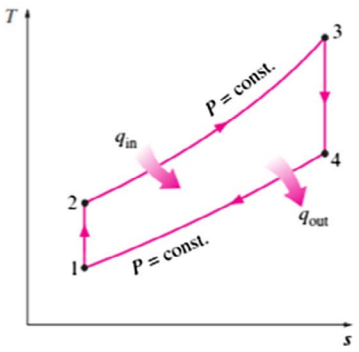

Fig. 4. Schematic diagram of CSSE cycle and the T-S diagram [28].

Table 2
Data validation results of the 25 kW_e CSSE compared with Abbas [3].

Parameter	The developed model	Abbas [3]
Aperture diameter, m	11.01	10.57
Aperture area, m^2	95.26	87.7
Focal length, m	7.34	7.45
Parabola height, m	1.03	N/A
Receiver area, m^2	0.088	0.2
Receiver diameter, cm	33.56	N/A
Rim angle	40	39
Optical efficiency	0.88	0.88
Mirror reflectivity	0.91	0.91
Cavity absorptivity	0.9	0.9
Operating temperature, °C	720	720
Displacement volume, cm^3	387.76	380
Bore and stroke, cm	5.5/4.081	5.5/4
No. of cylinders	4	4
Working fluid	H_2	H_2
Output power	25	25–27
Rotation speed	1800	1800
Peak net efficiency	26.3	29.4

3.1.1. Monatomic gases

The only chemical elements which are stable single atom molecules at standard temperature and pressure. These are Helium, Neon, Argon, Krypton, and Xenon. The mentioned gases are colorless, odorless, tasteless and expensive to get. These noble gases have weak interatomic force, and consequently have very low-melting and boiling points. Helium has several unique qualities when compared with other elements: its boiling and melting points are lower than those of any other known substance; it is the only element known to exhibit superfluidity; it is the only element that cannot be solidified by cooling under standard conditions. A pressure of 25 standard atmospheres (2500 kPa; 370 psi) must be applied at a temperature of 0.95 K (−272.20 °C; −457.96 °F) to convert it to a solid. The noble gases up to Xenon have multiple stable isotopes [25,26,30]. Table 3 illustrates some physical properties of the studied monatomic gases [30].

3.1.2. Diatomic gases

Diatomic molecules are molecules composed of only two atoms, of the same or different chemical elements. They are Hydrogen, Oxygen, Nitrogen, Fluorine, and Chlorine. Air, Hydrogen, and Nitrogen are considered in this study. Hydrogen gas is flammable and could be exploded under high pressure. Its uses are widely spread in all life applications. Air always used with Stirling engine. Table 4 illustrates the physical properties of the studied diatomic gases.

Table 4
Main physical properties of the addressed Diatomic gases [30].

Property	Air	H_2	N_2
Dynamic viscosity, Pa.s	1.849e−4	8.9154e−5	1.7805e−4
Gas density, kg/m^3	1.184	8.23e−2	1.145
Specific volume, m^3/kg	8.448e−1	11.983	8.734e−1
Thermal conductivity, W/m.K	2.6247e−2	1.8488e−1	2.5835e−2
Specific gravity	1	0.07	0.97

Note: All table data @ 25 °C and 1.013 bar.

3.1.3. Polyatomic gases

Polyatomic refers to the molecules or ions having two or more atoms. They are the molecules with two or more atoms. They do not have a positive or negative charge. In other words, these molecules are electrically neutral. (H_2SO_4, CH_3COOH, Na_2CO_3, NaCl, C_2H_4). In this study, CO_2, NH_3, CH_4, C_2H_2 are considered as working gases. There are so many physical and chemical differences between monatomic and polyatomic due to the difference in number of atoms. Table 5 illustrates some physical properties of the studied polyatomic gases.

3.2. Selection criteria

It was clear from literatures that Air, and/or Helium were widely used for solar dish Stirling engines. However; in this study, a spot light is focused on the effect of using different gases with different heat capacities for different engines. Different heat capacities have a great influence on the compression and presser ratios hence the efficiency. In this work, the selection of the working gas is performed based on some important criteria such as:

(a) The working fluid should be that of low viscosity to reduce compression losses. Using higher pressure or lower viscosity, or combinations thereof, could reduce the high mass flow required [1]. In

Table 3
Main physical properties of the addressed Monatomic gases [30].

Property	He	Ne	Ar	Kr	Xe
Dynamic viscosity, Pa.s	1.9846e−4	3.1113e−4	2.2624e−4	2.5132e−4	2.2985e−5
Gas density, kg/m^3	1.635e−1	8.242e−1	1.6335	3.4314	5.3937
Specific volume, m^3/kg	6.1166	1.2133	6.122e−1	2.914e−1	1.854e−1
Thermal conductivity, W/m.K	1.5531e−1	4.8084e−2	1.7746e−2	9.363e−3	5.535e−3
Specific gravity	0.14	0.7	1.38	2.9	4.56

Note: All table data @ 25 °C and 1.013 bar.

Table 5
Main physical properties of the addressed Polyatomic gases [30].

Property	CO_2	NH_3	CH_4	C_2H_2
Dynamic viscosity, Pa.s	1.4932e−4	1.0093e−4	1.1067e−4	1.0217e−4
Gas density, kg/m^3	1.8075	7.033e−1	6.567e−1	1.171
Specific volume, m^3/kg	5.532e−1	1.4218	1.5227	14.76
Thermal conductivity, W/m.K	1.6643e−2	2.4934e−2	3.3931e−2	2.2094e−2
Specific gravity	1.53	0.6	0.56	0.92

Note: All table data @ 25 °C and 1.013 bar.

general, polyatomic, and diatomic gives lower results related to the absolute viscosity.

(b) For the Stirling engine, specific heat capacity at constant volume is considered the key factor to judge the efficiency results due to Eqs. (4) and (5). However; the specific heat capacity at constant pressure is a vital role in the Brayton cycle related to each gas. Nonlinear correlations for each working gas are embedded within the program code and the values are changing with each model run according to the variation of the temperature. The considered correlations are shown Table 6 and correlations are explained in Appendix A.

(c) Changing the specific heat would change the compression and pressure ratios of both engines thence; the design aspects would change.

(d) High results of compression and pressure ratios would decrease the design aspects such as areas, diameters, etc. The highest pressure of working gas increases the speed of heat exchange as well. However; it may increase the engine cost due to the engine material to overcome high pressure stresses.

(e) Piston volume in the case of CSSE and mass flow rate in the case of CSBE.

(f) Maximum engine efficiency, maximum compression and pressure ratios.

(g) Minimum dish area and maximum dish concentration ratio.

(h) Minimum cost issues related to the engine and the dish area.

(i) Availability of the gases for industrial issues.

(j) Flammability, explosion, and environmental impact.

4. Results and discussions

In this part, data are run out for both engines (Stirling & Brayton) by the aid of REDS-CSGE model. All runs are executed at steady state conditions, and under the same operating conditions. The operational power range for both engines is fixed between 5 kW and 30 kW, and the temperature was in the range of 400–900 °C. Solar radiation, ambient temperature, and ambient pressure are fixed at 1000 W/m^2, 25 °C, and 1.03 bar respectively. For the CSSE, the model main target is to increase the power demanded from the engine or to reduce the design limits of the dish at the power load. Therefore; pinpointing the most reliable gas is becoming essential for the CSSE within these terms of concern:

- Compression and pressure ratios.
- Dish concentration ratio and focal length.
- Piston volume.
- Stirling and total plant efficiencies.
- Total plant area and costs.

Fig. 5 shows the effect of top cycle temperature on the specified terms. Increasing the top cycle temperature would increase all the dependent terms except the focal length which is desired to be reduced as a normal reduction result of design limits. Fig. 5a, b shows that C_2H_2 achieves higher results (compression ratio ranged from 10 to 23) compared against the rest gases however; CO_2 comes next with the range of 6 up to 11 of compression ratio parameter. Increasing the *CR* and *PR* parameters is favorable for CSSE. This effect of such increasing is reflected on the piston volume. Minimum values for piston volume are achieved by C_2H_2 meaning by this a reduction in design limits. Monatomic working gases give a general indication for the minimum results by the effect of top cycle temperature. The range of compression ratio wasn't exceeded over value 3. Diatomic gases such as air, comes next from bottom after Monatomic gases. Therefore; it is recommended from the current results to utilize the C_2H_2 working gas followed by CO_2, CH_4, then NH_3 (Polyatomic gages) regardless the flammability and high-pressure explosion issues. Increasing the top cycle temperature would increase the concentration ratio for the dish area hence; increasing the Stirling and total plant efficiencies (Fig. 5c, f). Fig. 6 shows the effect of compression ratio parameter on the CSSE dish area, Stirling efficiency, total plant cost, and piston volume parameters. For all working gases, increasing, the top cycle temperature hence, the compression ratio is quite favorable and desired. For dish area (Fig. 6a), optimum dish area was achieved at 78–80 m^2. Monatomic gases give the optimum area selection at $CR = 2.8$. The value of $CR = 5.77$–6 is remarkable for diatomic gases. Except C_2H_2, the *CR* of the polyatomic gases is found at $CR = 10$–11. Fig. 6b shows that increasing the *CR* would increase the CSSE efficiency hence, reducing the total plant costs (Fig. 6c). The effect of *CR* on a design parameter such as piston volume is noticed in Fig. 6d. It is obvious on the figure that C_2H_2 gives remarkable results. For Diatomic gases (Fig. 6d), CO_2 achieved remarkable results compared against the rest. However; NH_3 comes next and followed by air. Air and H_2 are considered little bit matched in their effect on the piston volume. Generally, C_2H_2 gives nearly 27 cm^3 at 800 °C ($CR = 23$) and 53 cm^3 at 400 °C ($CR = 13$). CH_4 comes next against the C_2H_2 by the range of 95 cm^3 down to 53 cm^3 at 800 °C ($CR = 12$). C_2H_2 gives attractive results on the *CR* because of its C_v, kJ/kg °C influence on Eqs. (4) and (5) $\Theta = \frac{1-\left(\frac{1}{\tau}\right)}{\frac{\eta_{SE}}{1-\left(\frac{1}{\tau}\right)}-1}$.....(4) $CR_{SE} = e^{\left(\frac{C_v}{R\times\Theta}\right)}$.....(5).

The generated power from the engine is considered a vital parameter for the reduction of the design limits. Fig. 7a, b, c shows the effect of top cycle temperature, and the generated power on the dish design limits. It is obvious from the figure that increasing the power would surly increase the design limits. Therefore; an optimized point should be considered for such behavior. Therefore; it is up to the decision makers or the designers to compare between large dish area and low engine volume related to the piston engine. In general, C_2H_2 would increase the CSSE performance and would reduce the piston volume

Table 6
The proposed working gases [25].

Working gas	[a]Specific heat capacity at constant pressure, C_p (kJ/kg °C)	[a]Specific heat capacity at constant volume, C_v (kJ/kg °C)
Monatomic gases		
Helium, He	5.19	3.12
Argon, Ar	0.52	0.312
Neon, Ne	1.053	0.618
Krypton, Kr	0.25	0.1488
Xenon, Xe	0.1615	0.097
Diatomic gases		
Air	1.0045	0.718
Hydrogen, H_2	14.29	10.16
Nitrogen, N_2	1.0376	0.743
Polyatomic gases		
Carbon dioxide, CO_2	0.8429	0.633
Ammonia, NH_3	2.239	1.66
Methane, CH_4	2.22	1.7
Acetylene, C_2H_2	1.694	1.37

[a] Note: Gases specific heat capacities are shown in Appendix A.

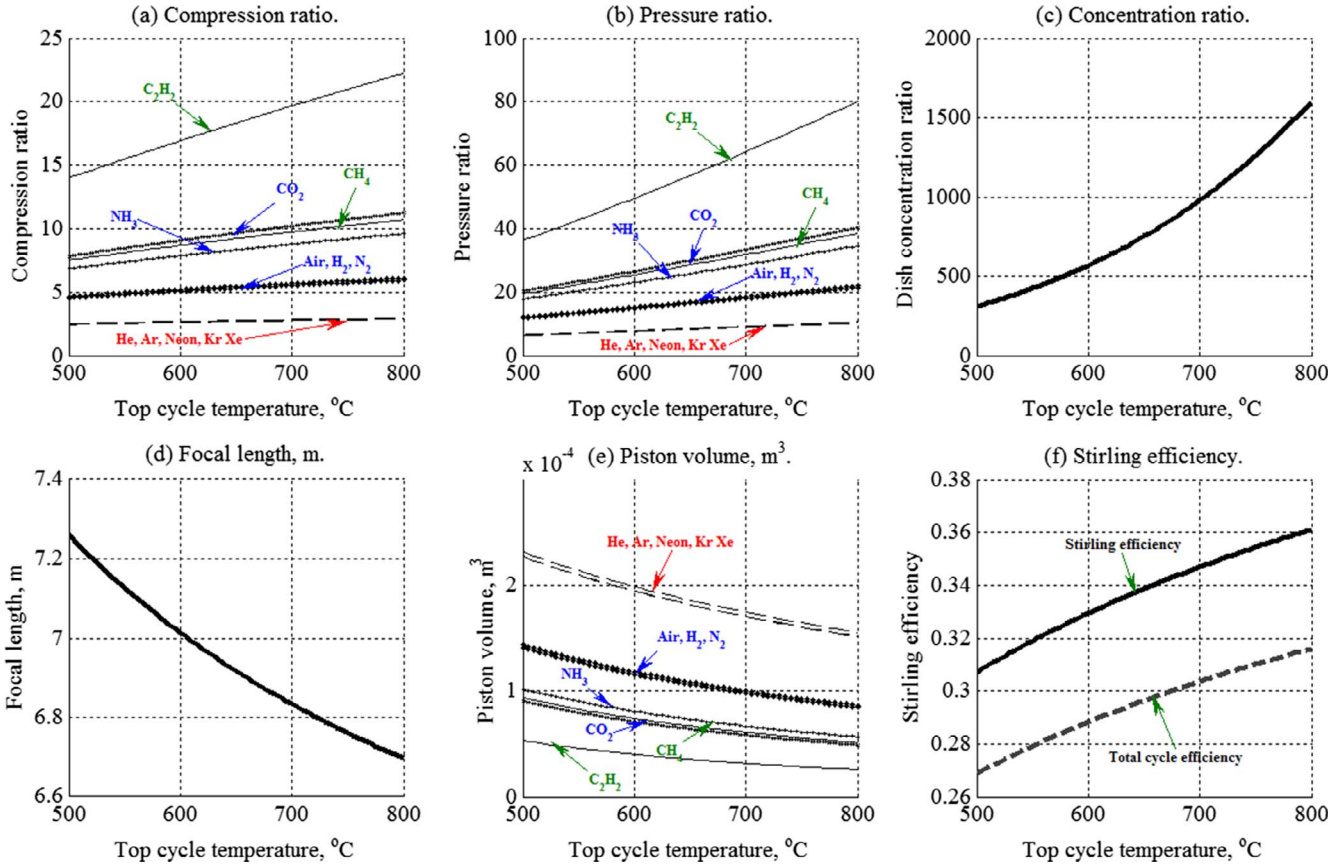

Fig. 5. Data results for CSSE model: (a) Compression ratio, (b) Pressure ratio, (c) Dish concentration ratio, (d) Focal length, (e) Piston volume, (f) Stirling efficiency.

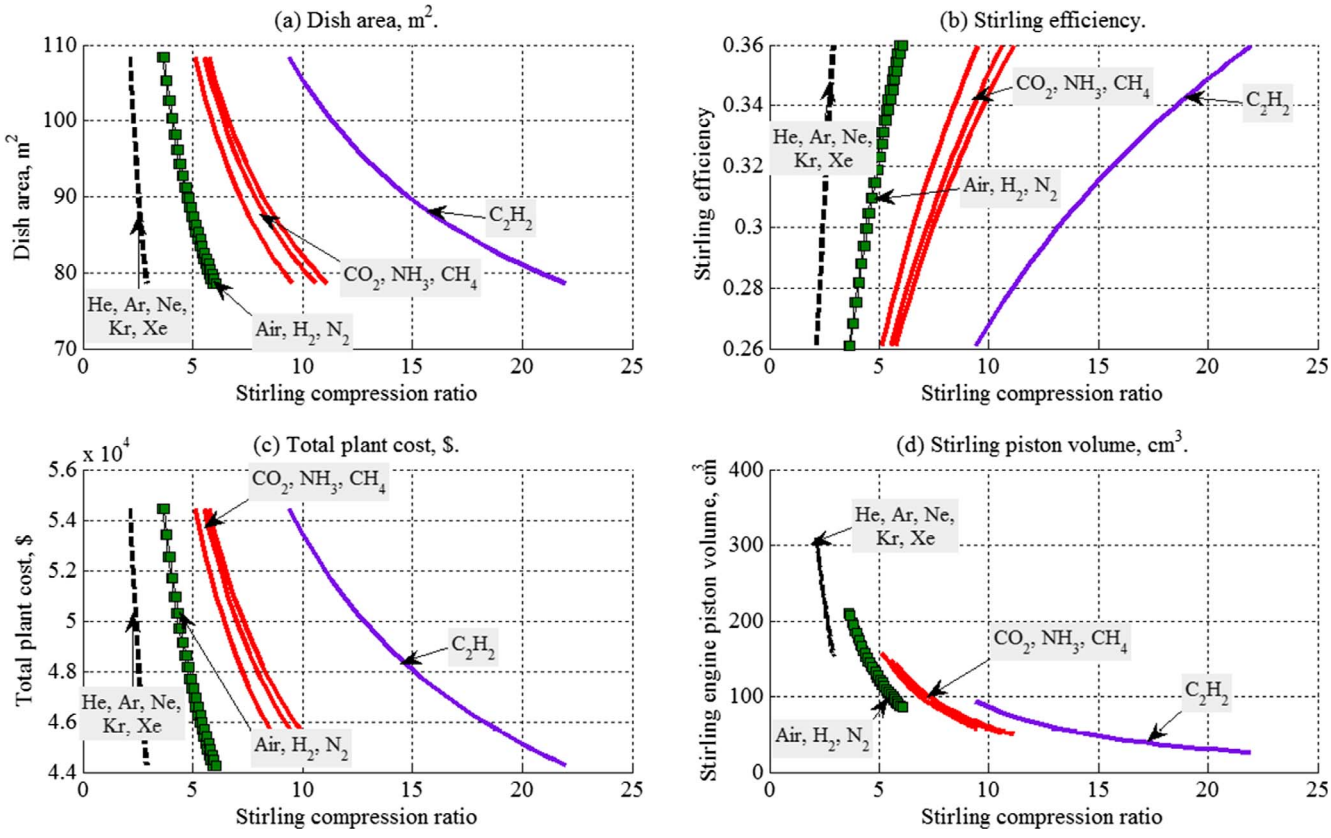

Fig. 6. Effect of Stirling compression ratio on the dish area, engine efficiency, total plant costs, and engine piston volume.

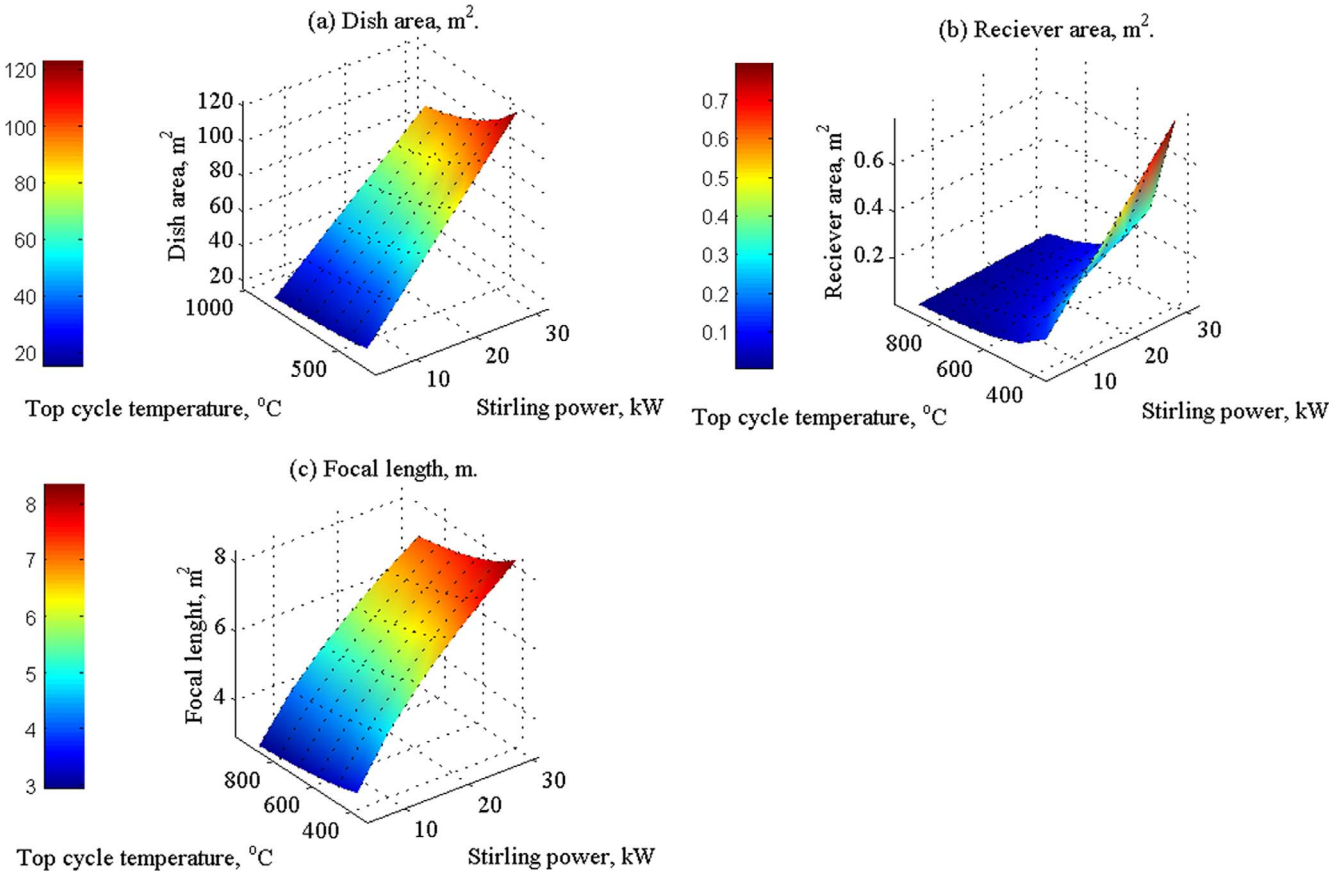

Fig. 7. The effect of top cycle temperature and the Stirling power on: (a) Dish area, (b) Receiver area, (c) Focal length.

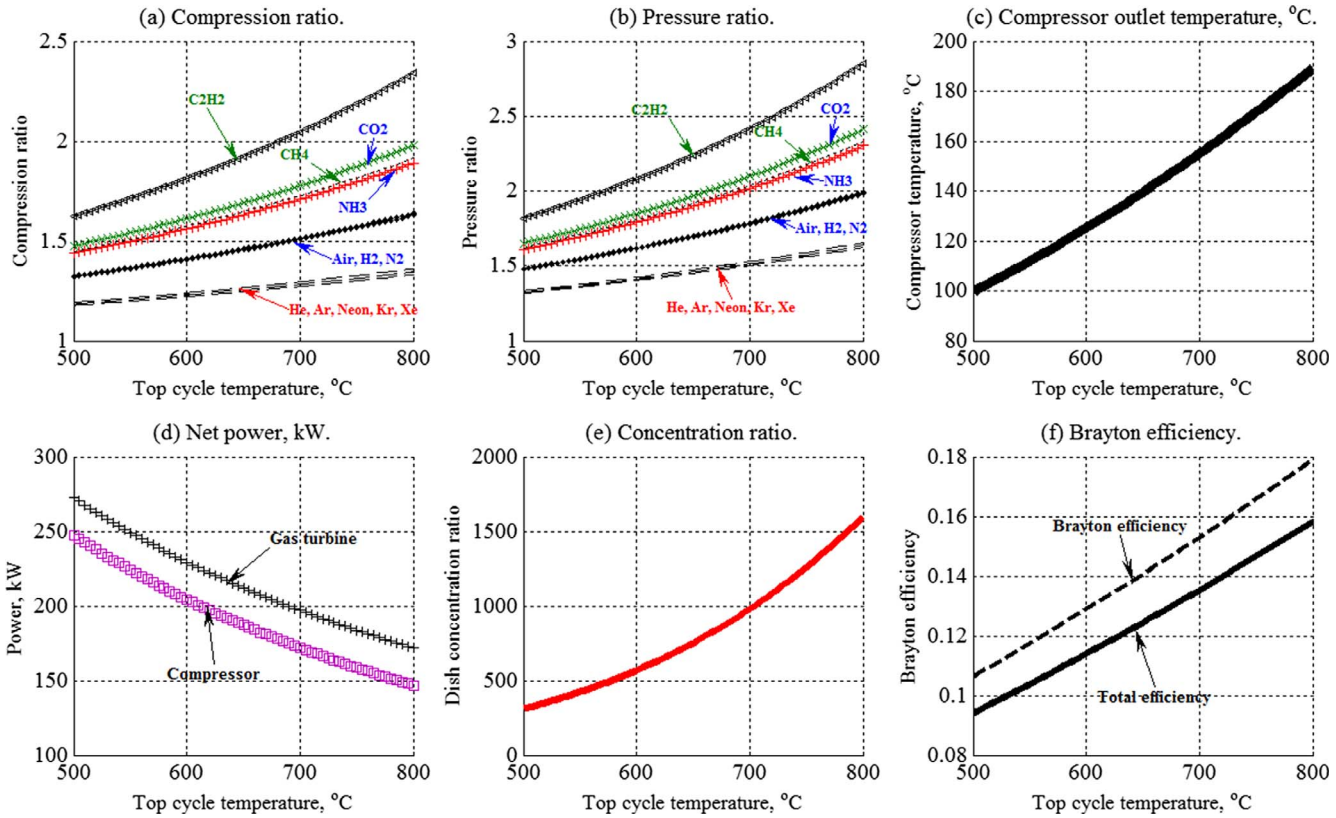

Fig. 8. Data results for CSBE model: (a) Compression ratio, (b) Pressure ratio, (c) Outlet compressor temperature, (d) Net power, (e) Dish concentration ratio, (f) Brayton efficiency.

with high compression and pressure ratios. Thence; it is recommended for the CSSE as a working gas regardless the safety issues. Fig. 8 shows the result of the top cycle temperature on the CSBE model. Increasing the top cycle temperature would increase all the relative parameters except the turbine and compressor powers. Fig. 8d shows that increasing the top cycle temperature would decrease the power load for the compressor and surly the turbine power however; the net power from the CSBE would be remained constant. The outlet compressor temperature is normally increased affected by the top cycle temperature (see Fig. 8c). Related to the compression and pressure ratios, C_2H_2 gives a notable result followed by the CO_2 compared against the rest of the gases (see Fig. 8a, b). Monatomic gases give the lowest values related to the terms of comparison. The Brayton cycle efficiency is increased by the increasing of the top cycle temperature term. It increased from 10.6% @ 400 °C up to 18% @ 800 °C leading by this increasing the plant total efficiency.

The Brayton engine efficiency is considered much lower while comparing against the Stirling engine. Fig. 9e shows the behavior of dish concentration ratio related to the CSBE temperature. The dish concentrated ratio is accustomed to increase by the increase of cycle temperature. In general, it is noticed that the compression and pressure ratios for the Brayton cycle are much lower than the Stirling cycle due to lower cycle efficiency against the Stirling. Fig. 9 shows the effect of top cycle temperature and the generated power on the design limits of the dish parabola. It is noticed from the 3D curves that increasing the power load would increase the design limits even the gas turbine rotational speed. It is pointed in Fig. 9d that the optimum turbine speed was at the range of 2500–3000 r.p.m. The behavior is quite noticed that the dish area has increased from 60 m^2 @ 5 kW up to 400 m^2 @ 30 kW. The same behavior is normally noticed on the receiver area. The generated power by gas turbine is also increased meaning by this increasing the total plant efficiency. Generally, increasing the power would increase the design limits which are not favorable for Brayton cycle with 20% of cycle efficiency. For maximum power and low dish area, 150–200 m^2 would be the optimum value which is considered much larger than the CSSE case.

Fig. 10 behavior shows the effect of compression ratio parameter on the dish area, engine efficiency, total plant costs, and cycle mass flow rate. Fig. 10a shows that by increasing the pressure ratio the dish area is decreasing as well. For all cases, the pressure ratio for the CSBE wasn't exceeded over PR = 3. Dish area of 160 m^2 is considered an optimum value which surly much higher (not favorable) than the operation of CSSE case. In case of operating conditions at $PR = 2$, CO_2, NH_3, and CH_4 are favorable. For $PR > 2.5$, C_2H_2 is favorable working gas. Fig. 10b shows that increasing the PR would increase the cycle efficiency. The optimum cycle efficiency was obtained at 16% which is much lower than the CSSE case. That result is reflected on the total plant costs (see Fig. 10c).

Fig. 10d shows that high rates of mass flow is remarkable by monatomic gases however; the PR is not exceeding over 1.5. Generally, polyatomic gases give higher values of pressure ratio with respect to C_2H_2 ($1.5 < PR < 3$). It is noticed that Brayton engine (CSBE) achieved lower results for the engine efficiency reached up to 16% against 37.6% for the CSSE. This is considered a huge advantage to the CSSE which causes a reduction in dish area, receiver area, focal length, and surly the weight of the system. Furthermore; the C_2H_2 achieves remarkable results for both engines with an advantage to the CSSE operational case. Therefore; C_2H_2, CO_2, and NH_3 are recommended for CSBE operation according to their wide range of PR. That is referring to the influence of specific heat capacity at constant pressure (C_p, kJ/kg °C) on the PR ($r_p = \left(\frac{1}{1-\eta_{BE_a}}\right)^{\left(\frac{\gamma}{\gamma-1}\right)}$.....(23)). It is quite evidence from Eq. (23) that gases with high values of adiabatic index (γ) would give lower values of PR. That's explained why Helium and monatomic gases give lowest values of PR. For example, the adiabatic index for Helium is $\gamma = 16.6312$ hence; giving minimum values for the PR. C_2H_2 with $\gamma = 1.241$ would result the highest value of the PR and the same for polyatomic gases. CO_2 comes after the C_2H_2 with an adiabatic index

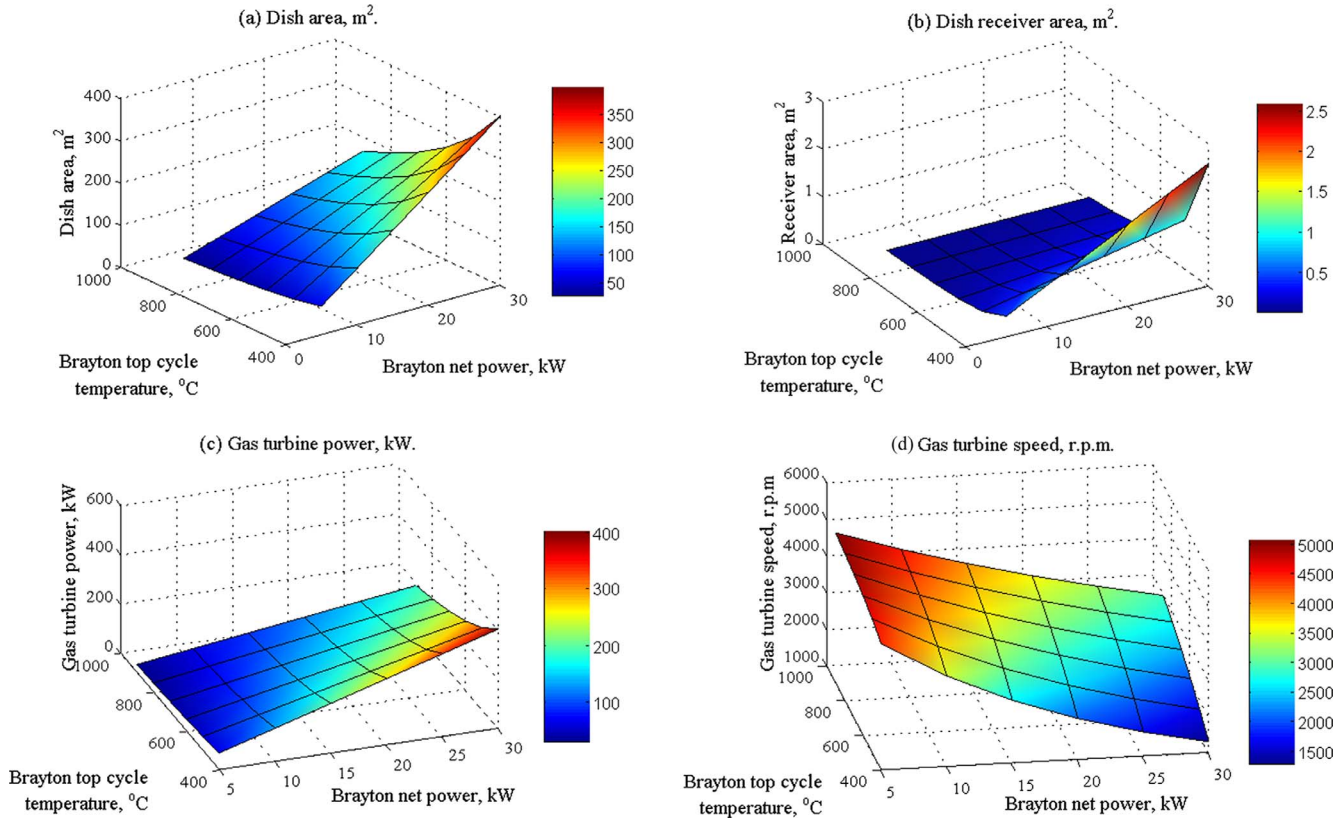

Fig. 9. Effect of top cycle temperature and the CSBE generated power on: (a) Dish area, (b) Receiver area, (c) Gas turbine power, (d) Gas turbine speed.

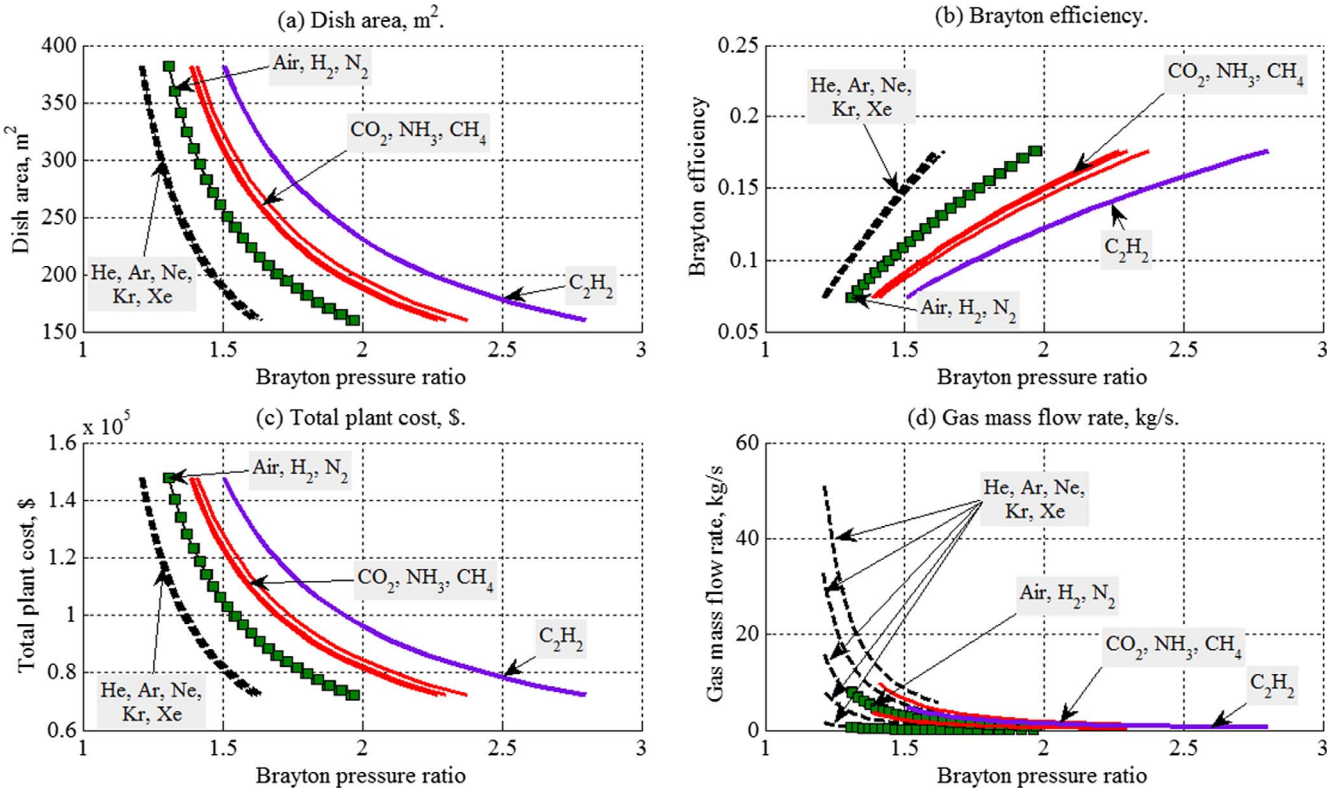

Fig. 10. Effect of CSBE pressure ratio on: (a) Dish area, (b) Efficiency, (c) Total plant costs, (d) Cycle mass flow rate.

equal to $\gamma = 1.3318$.

Fig. 11 shows the effect of power increasing on the total plant area and the total plant cost parameter. It is pinpointed from Fig. 11 that CSBE achieves higher design limits values against the CSSE under the operation of C_2H_2 working gas. For 90 MW_e total power plant, CSSE is leading by 44% related to the reduction in total plant area, m^2. CSSE also gives a remarkable result for 90 MW_e based on the total plant costs by saving 3–5% of the total costs against the CSBE. In general, C_2H_2 for

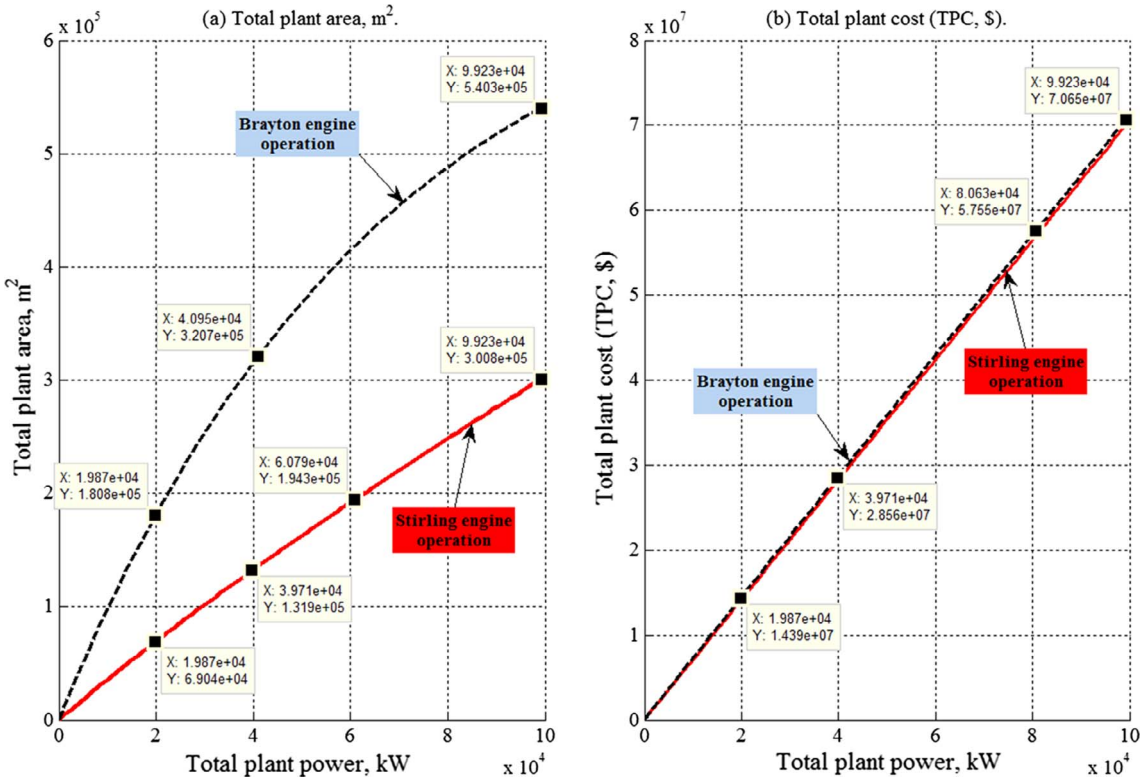

Fig. 11. Data comparisons for CSSE vs. CSBE related to total plant area and total plant costs.

Table 7
Data comparisons for CSBE against CSSE (C_2H_2 operation).

Parameter	CSBE	CSSE
Total power, MW_e	100	100
Engine power, kW_e	25	25
Top cycle temperature, °C	800	800
Lower cycle temperature, °C	25	25
Rim angle	40	40
Total plant area, m^2	6.3126e5	3.131e5
Total dish area, m^2	157.8	78.27
Receiver area, m^2	0.098	0.05
Focal length, m	9.46	6.7
Parabola height, m	1.327	0.94
Number of dishes, #	4000	4000
Total efficiency, %	15.84	32
Compression/pressure ratio	2.342/2.853	22.24/80
Max volume/Min volume, m^3/kg	0.9292/0.3968	0.93/0.04178
Total plant costs, $	7.143e7	7.061e7

Notes:
- Solar radiation, $W/m^2 = 1000$.
- Generator efficiency, % = 95.
- Receiver efficiency, % = 70–94 (according to temperature variation).
- Dish mirror efficiency, % = Polymeric-lm, nonmetal, 98% with 2% emissive.
- Absorptivity of the receiver, % = 94.

CSSE is quite remarkable and favorable in order to achieve higher results related to the compression and pressure ratios. CO_2 comes next related to the terms of comparison.

Table 7 shows the data results related to a 100 MW_e case study operated by CSBE vs. CSSE based on C_2H_2 working gas. It is quite evidence from Table 7 that CSSE gives lower area against CSBE and the same behavior is found related to the total plant costs, $. Fig. 12 shows the effect of power increasing on the total cycle efficiency for both engines. It is clear from Fig. 12 that CSSE gives the highest remarkable results. It almost achieves three times greater than the CSBE. The same effect is normally noticed on the total dish area for both cases. High efficiency means low dish area with respect to high power production. That's because the total cycle efficiency is affected by the dish area as presented in Eqs. (8) and (9). The dish area is considered an important factor that affecting on the total cycle efficiency. The effect of top cycle temperature and receiver efficiency is shown in Fig. 13. Increasing the top cycle temperature would decrease the dish area and the total plant cost. Also, increasing the receiver efficiency would cause the same effect on the design limits and the cost parameters. However; increasing the top cycle temperature would decrease the receiver efficiency as well. Therefore; the behavior shown in Fig. 12 concludes the situation for dish area and total plant cost. Related to dish area, it is shown that CSBE gives high and unremarkable results against the CSSE (450 m^2 vs 130 m^2) i.e. extra cost. Total plant cost parameter is also achieved the same behavior. CSSE gives slightly remarkable results vs the CSBE with the operation of C_2H_2. According to the C_v, kJ/kg °C of the C_2H_2, this gas gives superb results followed by the CO_2 however; its flammable with self-ignition temperature at 300 °C.

5. Recommendations

Generally; CSSE gives remarkable results against the CSBE cycle due to the effect of thermal efficiency of the Stirling engine while comparing at the same temperature level. Based on *CR*, monatomic gases give minimum values ($1.5 < CR < 2.86$). Diatomic gases come in the second rank by the range of $2.8 < CR < 5.7$. Polyatomic gases except the C_2H_2 come in the third rank by achieving a range of $5.5 < CR < 11$. C_2H_2 achieved superb results according the *CR* with a range of $10 < CR < 22$. Furthermore; the same behavior was achieved regarding to the operation of CSBE based on the *PR* parameter. C_2H_2 gives remarkable results according to the *PR* ($1.5 < PR < 2.66$). From all gases, hydrogen has the highest heat capacity. However; hydrogen is dangerous because the possibility of explosion and burning in the air is very high. Hydrogen makes a relatively wide range of explosion mixture in air between 4% and 74%. Helium is much more expensive than hydrogen, however; helium has very low chemical reactivity and is included to the noble gases. CO_2 comes next after C_2H_2 and followed by the CH_4 and NH_3 respectively. Regarding to safety issues, CO_2, N_2, and Air are dominant, because, C_2H_2, CH_4, are highly flammable and can be exploded at high pressure. According to monatomic gases, they are too expensive with low *CR* and *PR* comparing against the rest of the gases. Therefore, it is up to the designers' decision by taking safety in their accounts, CO_2 is favorable with *CR* up to 11. Fig. 14 shows the comparison between all gases according to the selection of the *CR* and *PR* ranges based on both engines (CSSE & CSBE). The designer has to select the category of the *CR* and/or *PR* in order to be able to decide which gas should be utilized with the CSGE. For low *CR* and *PR*, monatomic gases give optimum results with high rank of safety with efficiency range not exceeding over 26% for CSSE and 7.5–15% for CSBE operation. Diatomic gases come next with a range of 31% for CSSE and 15–17.5% for CSBE. Finally, polyatomic gases (in general) gives the highest level of engine efficiency with a range of 32–36% for the CSSE and 17.5% for CSBE. At the same time, polyatomic gases are not safe and highly flammable. Despite of the *CR* and the *PR* results, the self-ignition temperature of the H_2, NH_3, CH_4,

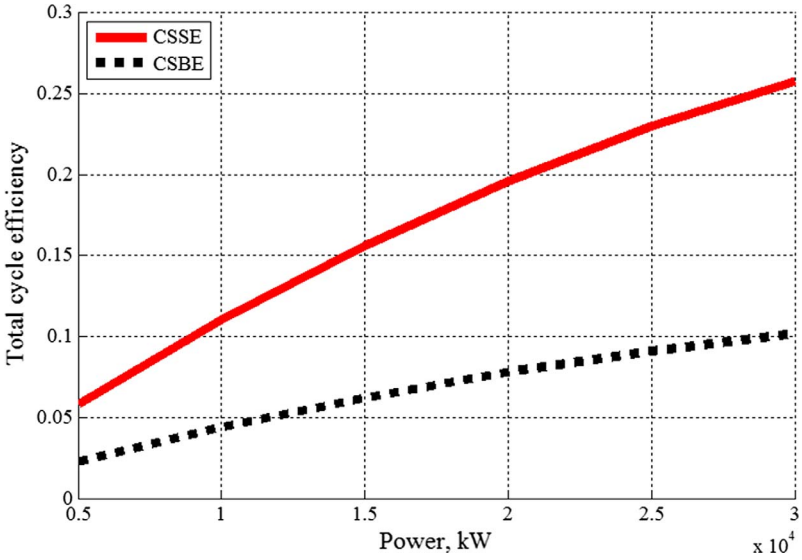

Fig. 12. Effect of cycle power on the cycle total efficiency for both engines, CSSE & CSBE.

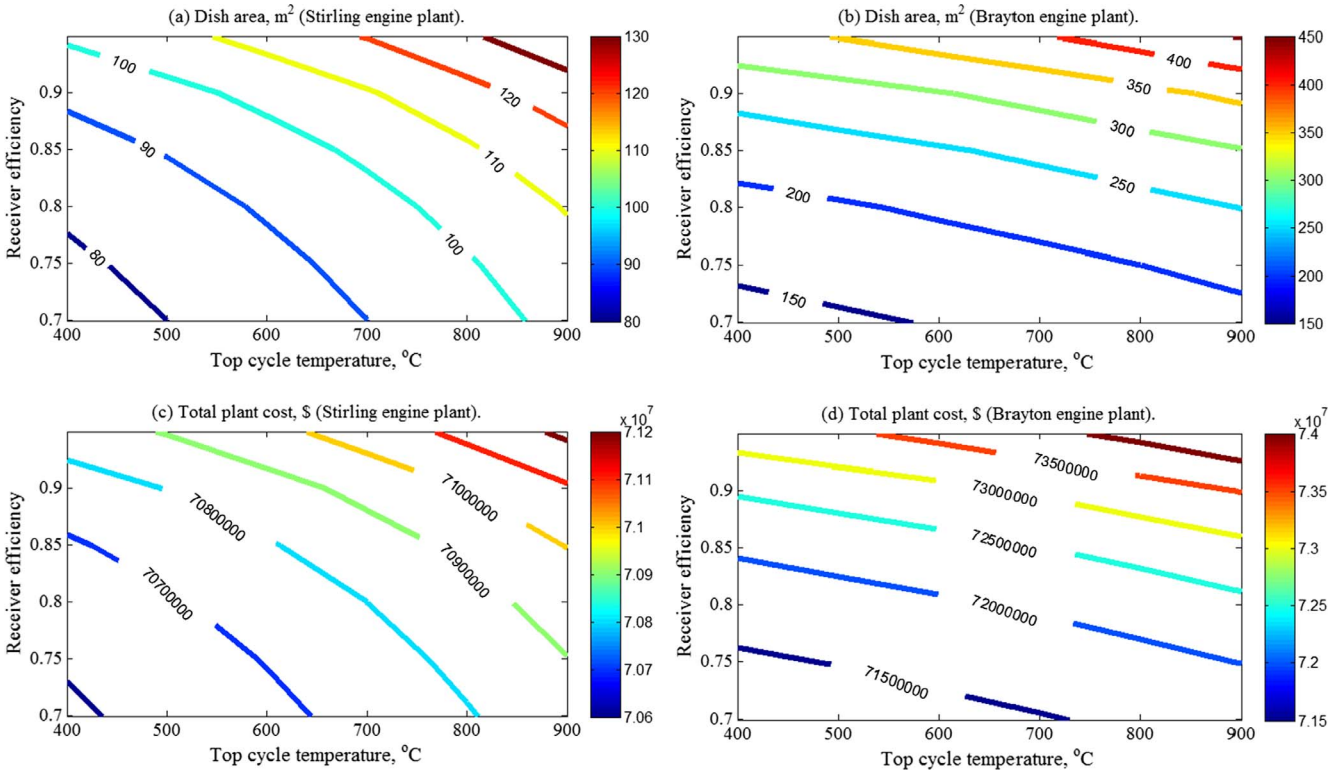

Fig. 13. Effect of receiver efficiency on solar dish area, m^2 and TPC, $ for both plants (CSSE & CSBE).

Parameter:	Value:	CSSE choice													
	CR	He	Ar	Ne	Kr	Xe	Air	H_2	N_2	CO_2	NH_3	CH_4	C_2H_2	Recommended gas
Dish area, m^2	2.5	✓ 78	✓ 78	✓ 78	✓ 78	✓ 78	✗ 0	✗ 0	✗ 0	✗ 0	✗ 0	✗ 0	✗ 0	Monatomic
	5	✗ 0	✗ 0	✗ 0	✗ 0	✗ 0	✓ 83	✓ 83	✓ 83	✓ 109	✓ 109	✗ 0	Diatomic	
	8	✗ 0	✗ 0	✗ 0	✗ 0	✗ 0	✗ 0	✗ 0	✗ 0	✓ 85	✓ 85	✓ 85	✗ 0	CO_2, NH_3, CH_4
	10	✗ 0	✗ 0	✗ 0	✗ 0	✗ 0	✗ 0	✗ 0	✗ 0	✓ 80	✓ 80	✓ 80	✓ 105	CO_2, NH_3, CH_4
	15	✗ 0	✗ 0	✗ 0	✗ 0	✗ 0	✗ 0	✗ 0	✗ 0	✗ 0	✗ 0	✗ 0	✓ 90	C_2H_2
	22	✗ 0	✗ 0	✗ 0	✗ 0	✗ 0	✗ 0	✗ 0	✗ 0	✗ 0	✗ 0	✗ 0	✓ 78	C_2H_2
	CR	He	Ar	Ne	Kr	Xe	Air	H_2	N_2	CO_2	NH_3	CH_4	C_2H_2	Recommended gas
Efficiency, %	2.5	✓ 26	✓ 26	✓ 26	✓ 26	✓ 26	✗ 0	✗ 0	✗ 0	✗ 0	✗ 0	✗ 0	✗ 0	Monatomic
	5	✗ 0	✗ 0	✗ 0	✗ 0	✗ 0	✓ 31	✓ 31	✓ 31	✓ 26	✓ 26	✗ 0	Diatomic	
	8	✗ 0	✗ 0	✗ 0	✗ 0	✗ 0	✗ 0	✗ 0	✗ 0	✓ 32	✓ 32	✓ 32	✗ 0	CO_2, NH_3, CH_4
	10	✗ 0	✗ 0	✗ 0	✗ 0	✗ 0	✗ 0	✗ 0	✗ 0	✓ 34	✓ 34	✓ 34	✓ 26.5	CO_2, NH_3, CH_4
	15	✗ 0	✗ 0	✗ 0	✗ 0	✗ 0	✗ 0	✗ 0	✗ 0	✗ 0	✗ 0	✗ 0	✓ 33	C_2H_2
	22	✗ 0	✗ 0	✗ 0	✗ 0	✗ 0	✗ 0	✗ 0	✗ 0	✗ 0	✗ 0	✗ 0	✓ 36	C_2H_2
Parameter:	Value:	CSBE choice													
	PR	He	Ar	Ne	Kr	Xe	Air	H_2	N_2	CO_2	NH_3	CH_4	C_2H_2	Recommended gas
Dish area, m^2	1.25	✓ 300	✓ 300	✓ 300	✓ 300	✓ 300	✗ 0	✗ 0	✗ 0	✗ 0	✗ 0	✗ 0	✗ 0	Monatomic
	1.5	✗ 160	✗ 160	✗ 160	✗ 160	✗ 160	✓ 250	✓ 250	✓ 250	✓ 300	✓ 300	✓ 300	✓ 355	Diatomic
	1.75	✗ 0	✗ 0	✗ 0	✗ 0	✗ 0	✓ 160	✓ 160	✓ 160	✓ 245	✓ 245	✓ 245	✓ 260	CO_2, NH_3, CH_4
	2	✗ 0	✗ 0	✗ 0	✗ 0	✗ 0	✓ 155	✓ 155	✓ 155	✓ 200	✓ 200	✓ 200	✓ 230	CO_2, NH_3, CH_4
	2.3	✗ 0	✗ 0	✗ 0	✗ 0	✗ 0	✗ 0	✗ 0	✗ 0	✓ 155	✓ 155	✓ 155	✓ 170	CO_2, NH_3, CH_4
	2.5	✗ 0	✗ 0	✗ 0	✗ 0	✗ 0	✗ 0	✗ 0	✗ 0	✗ 0	✗ 0	✗ 0	✓ 160	C_2H_2
	2.55	✗ 0	✗ 0	✗ 0	✗ 0	✗ 0	✗ 0	✗ 0	✗ 0	✗ 0	✗ 0	✗ 0	✓ 155	C_2H_2
	PR	He	Ar	Ne	Kr	Xe	Air	H_2	N_2	CO_2	NH_3	CH_4	C_2H_2	Recommended gas
Efficiency, %	1.25	✓ 7.5	✓ 7.5	✓ 7.5	✓ 7.5	✓ 7.5	✗ 0	✗ 0	✗ 0	✗ 0	✗ 0	✗ 0	✗ 0	Monatomic
	1.5	✓ 15	✓ 15	✓ 15	✓ 15	✓ 15	✓ 10	✓ 10	✓ 10	✓ 8.5	✓ 8.5	✓ 8.5	✓ 7.5	Diatomic
	1.55	✗ 0	✗ 0	✗ 0	✗ 0	✗ 0	✓ 15	✓ 15	✓ 15	✓ 12	✓ 12	✓ 12	✓ 10	CO_2, NH_3, CH_4
	2	✗ 0	✗ 0	✗ 0	✗ 0	✗ 0	✓ 17.5	✓ 17.5	✓ 17.5	✓ 15	✓ 15	✓ 15	✓ 12	CO_2, NH_3, CH_4
	2.3	✗ 0	✗ 0	✗ 0	✗ 0	✗ 0	✗ 0	✗ 0	✗ 0	✓ 16	✓ 16	✓ 16	✓ 13.5	CO_2, NH_3, CH_4
	2.5	✗ 0	✗ 0	✗ 0	✗ 0	✗ 0	✗ 0	✗ 0	✗ 0	✗ 0	✗ 0	✗ 0	✓ 15.5	C_2H_2
	2.55	✗ 0	✗ 0	✗ 0	✗ 0	✗ 0	✗ 0	✗ 0	✗ 0	✗ 0	✗ 0	✗ 0	✓ 16.5	C_2H_2
General specifications for the gases														
		He	Ar	Ne	Kr	Xe	Air	H_2	N_2	CO_2	NH_3	CH_4	C_2H_2	Recommended gas
Flammability		✗	✗	✗	✗	✗	✗	✓	✗	✗	✓	✓	✓	Monatomic, Air, N_2, CO_2
Explosion		✗	✗	✗	✗	✗	✗	✓	✗	✗	✓	✓	✓	Monatomic, Air, N_2, CO_2
Autoignition temperature, °C		✗ 0	✗ 0	✗ 0	✗ 0	✗ 0	✗ 0	✓ 500	✗ 0	✗ 0	✓ 651	✓ 537	✓ 300	Monatomic, Air, N_2, CO_2

Fig. 14. Data results for all working gases based on dish area, and engine efficiency.

C_2H_2 are 500, 651, 537, and 300 °C respectively. Therefore; and considering the safety issues, the designer selection should be kept up with the following:

- Engine selection: CSSE (Concentrated Solar Stirling Engine).
- *CR* range.
- 4–11.
- Working gas: CO_2.

6. Conclusion

Increasing the efficiency of the concentrated solar gas engine (CSGE) is considered a very important issue till today. Increasing engine performance means reducing the design limits thence; reducing the total weight and costs. The problem was how to increase the gained power from the solar dish engines. Solar dish engines have massive advantages concluded into:

- Tracking with the sun means working hours' stability.
- High receiver efficiency.
- High mirror efficiency.

However; there is a massive defect in the engine itself which drops the total efficiency down to unacceptable limits (from 95% receiving efficiency to 22% total efficiency). The aim of this work is focused on the engine, how can we increase the engine efficiency. Therefore; in this work, examining the effect of different working gases on the efficiency of two types of gas engines is performed. The Effect was to discover of twelve gases on several parameters such as size, efficiency, engine size, temperature, compression and pressure ratios, etc. The gases are divided into main three categories based on their behavior and atomic number which are:

- Monatomic gases (Helium-He, Argon-Ar, Neon-Ne, Krypton-Kr, Xenon-Xe).
- Diatomic gases (Air, Hydrogen-H_2, Nitrogen-N_2).
- Polyatomic gases (Carbon dioxide-CO_2, Ammonia-NH_3, Methane-CH_4, Acetylene-C_2H_2).

The proposed gases are used for both cycles (Stirling and Brayton) for solar dish operation. Among these gases, C_2H_2 followed by CO_2 gives remarkable results against the conventional operation (Air, H_2, He, N_2). Both gases achieved higher compression and pressure ratios regardless the C_2H_2 safety issues. In general; concentrated solar Stirling gas engine (CSSE) gives a remarkable result against the concentrated solar Brayton engine (CSBE) under the same working gas and the same operating conditions. CSSE achieves more than 3–5% cost reduction against CSBE with nearly 44% reduction in total plant area due to less efficiency of the CSBE against the CSSE (10% vs. 26%). According to the engine efficiency, compression ratio and safety issues, CO_2, NH_3, and Air gases are found more likely to be used and considered for CSSE instead of CSBE with a huge advantage to the CO_2. Their range of compression ratio was found as 4–11. The specific heat capacity is found a vital role which affecting on the *CR* and *PR*. Gases with lowest adiabatic index (C_2H_2, CO_2, CH_4, NH_3) give the highest value of *CR* and *PR*. C_2H_2 achieved remarkable results based on efficiency, compression ratio and dish area however; it is found too dangerous to be used in the gas engines because it is flammable and has a low self-ignition point.

Appendix A. Working gases

Gas	C_p, kJ/kg°C	R, kJ/kg°C
Helium, He [26] Molecular weight= 4.0026g/mol	$C_p = (A+B*t+C*t^2+D*t^3+E/t^2)/4.0026$ t (K): 298 - 6000 A: 20.78603 B: 4.850638×10^{-10} C: -1.582916×10^{-10} D: 1.525102×10^{-11} E: 3.196347×10^{-11}	2.08
Argon, Ar [26] Molecular weight= 39.948g/mol	$C_p = (A+B*t+C*t^2+D*t^3+E/t^2)/39.948$ t (K): 298 - 6000 A: 20.78600 B: 2.825911×10^{-7} C: -1.464191×10^{-7} D: 1.092131×10^{-8} E: -3.661371×10^{-8}	0.208
Neon, Ne [26] Molecular weight= 20.1797g/mol	$C_p = (A+B*t+C*t^2+D*t^3+E/t^2)/20.1797$ t (K): 298 - 6000 A: 20.78603 B: 4.850638×10^{-10} C: -1.582916×10^{-10} D: 1.525102×10^{-11} E: 3.196347×10^{-11}	0.412
Krypton, Kr [26] Molecular weight= 83.798 g/mol	$C_p = (A+B*t+C*t^2+D*t^3+E/t^2)/83.798$ t (K): 298 - 6000 A: 20.78603 B: 4.850638×10^{-10} C: -1.582916×10^{-10} D: 1.525102×10^{-11} E: 3.196347×10^{-11}	0.1022
Xenon, Xe [26] Molecular weight= 131.293g/mol	$C_p = (A+B*t+C*t^2+D*t^3+E/t^2)/131.293$ t (K): 298 - 6000 A: 20.78600 B: 7.449320×10^{-7} C: -2.049401×10^{-7} D: 1.066661×10^{-8} E: 2.500261×10^{-8}	0.0646
Air [27] Molecular weight= 28.97g/mol	$C_p = 1.137-0.09317*\cos(t*0.002094)-0.07036*\sin(t*0.002094)-0.01959*\cos(2*t*0.002094)-0.01042*\sin(2*t*0.002094)$ t (K)	0.287

Hydrogen, H_2 [26]
Molecular weight= 2.01588g/mol

$C_p=(A+B*t+C*t^2+D*t^3+E/t^2)/2.01588$

t (K)	298 - 1000	1000 - 2500	2500 - 6000
A	33.066178	18.563083	43.413560
B	-11.363417	12.257357	-4.293079
C	11.432816	-2.859786	1.272428
D	-2.772874	0.268238	-0.096876
E	-0.158558	1.977990	-20.533862

4.12

Nitrogen, N_2 [26]
Molecular weight= 28.0134g/mol

$C_p=(A+B*t+C*t^2+D*t^3+E/t^2)/28.0134$

t (K)	100 - 500	500 - 2000	2000 - 6000
A	28.98641	19.50583	35.51872
B	1.853978	19.88705	1.128728
C	-9.647459	-8.598535	-0.196103
D	16.63537	1.369784	0.014662
E	0.000117	0.527601	-4.553760

0.297

Carbon dioxide, CO_2 [26]
Molecular weight= 44.0095g/mol

$C_p=(A+B*t+C*t^2+D*t^3+E/t^2)/44.0095$

t (K)	298 - 1200	1200 - 6000
A	24.99735	58.16639
B	55.18696	2.720074
C	-33.69137	-0.492289
D	7.948387	0.038844
E	-0.136638	-6.447293

0.189

Ammonia, NH_3 [26]
Molecular weight= 17.0305g/mol

$C_p=(A+B*t+C*t^2+D*t^3+E/t^2)/17.0305$

t (K)	298 - 1400	1400 - 6000
A	19.99563	52.02427
B	49.77119	18.48801
C	-15.37599	-3.765128
D	1.921168	0.248541
E	0.189174	-12.45799

0.53

Methane, CH_4 [26]
Molecular weight= 16.0425g/mol

$C_p=(A+B*t+C*t^2+D*t^3+E/t^2)/16.0425$

t (K)	298 - 1300	1300 - 6000
A	-0.703029	85.81217
B	108.4773	11.26467
C	-42.52157	-2.114146
D	5.862788	0.138190
E	0.678565	-26.42221

0.518

Acetylene, C_2H_2 [26]
Molecular weight= 26.0373g/mol

$C_p=(A+B*t+C*t^2+D*t^3+E/t^2)/26.0373$

t (K)	298 - 1100	1100 - 6000
A	40.68697	67.47244
B	40.73279	11.75110
C	-16.17840	-2.021470
D	3.669741	0.136195
E	-0.658411	-9.806418

0.319

Note: $R = C_p - C_v, \gamma = \frac{C_p}{C_v}$

Appendix B. Brayton engine optimum efficiency

The ideal cycle efficiency is obtained as;

$$\eta_{th} = 1-\sqrt{\frac{T_{min}}{T_{max}}} \tag{B.1}$$

For actual cycle; the compressor power is obtained as;

$$W_{comp} = \frac{C_p(T_{2s}-T_1)}{\eta_C} \tag{B.2}$$

where η_c is the compressor efficiency and $\frac{T_{2s}}{T_1} = r_p^{\frac{\gamma-1}{\gamma}}$, then;

$$W_{comp} = \frac{C_p\left(T_1.\, r_p^{\frac{\gamma-1}{\gamma}}-T_1\right)}{\eta_C} \tag{B.3}$$

The turbine power is calculated as;

$$W_T = \eta_T.\, C_p(T_3-T_{4s}) \tag{B.4}$$

where $\frac{T_{4s}}{T_3} = \frac{1}{r_p^{\frac{\gamma-1}{\gamma}}}$ and η_T is the turbine efficiency and the turbine power is written as follows

$$W_T = \eta_T.\, C_p\left(T_3-\frac{T_3}{r_p^{\frac{\gamma-1}{\gamma}}}\right) \tag{B.5}$$

And the net power is written follows;

$$W_{net} = W_T-W_{comp} = \eta_T.\, C_p\left(T_3-\frac{T_3}{r_p^{\frac{\gamma-1}{\gamma}}}\right)-\frac{C_p\left(T_1.\, r_p^{\frac{\gamma-1}{\gamma}}-T_1\right)}{\eta_C} \tag{B.6}$$

To obtain the optimum net power with respect to the pressure ratio,

$$\frac{\delta W_{net}}{\delta r_p} = \eta_T.\, C_p T_3.\, \frac{\gamma-1}{\gamma}.\, r_p^{-\frac{(\gamma-1)}{\gamma}-1}-\frac{C_p}{\eta_C}.\, T_1.\, \frac{\gamma-1}{\gamma}.\, r_p^{\frac{\gamma-1}{\gamma}-1} = 0.0 \tag{B.7}$$

$$\eta_T.\, T_3.\, r_p^{-\frac{(2\gamma-1)}{\gamma}} = \frac{1}{\eta_C}.\, T_1.\, r_p^{\frac{-1}{\gamma}} \tag{B.8}$$

$$\eta_T.\, T_3 = \frac{1}{\eta_C}.\, T_1.\, r_p^{\frac{-1}{\gamma}+\frac{(2\gamma-1)}{\gamma}} \tag{B.9}$$

$$\eta_C.\, \eta_T.\, \frac{T_3}{T_1} = r_p^{\frac{2(\gamma-1)}{\gamma}} \tag{B.10}$$

$$\sqrt{\frac{T_3}{T_1}\eta_T\eta_C} = r_p^{\frac{(\gamma-1)}{\gamma}} \tag{B.11}$$

$$r_p = \left(\frac{T_3}{T_1}\eta_T\eta_C\right)^{\frac{\gamma}{2(\gamma-1)}} \tag{B.12}$$

The optimum net power is then obtained as;

$$W_{net.optimum} = W_T-W_{Comp} = \eta_T.\, C_p\left(T_3-\frac{T_3}{\sqrt{\frac{T_3}{T_1}\eta_T\eta_C}}\right)-\frac{C_p\left(T_1.\, \sqrt{\frac{T_3}{T_1}\eta_T\eta_C}-T_1\right)}{\eta_C} \tag{B.13}$$

And the heat addition is calculated as;

$$Q_{add} = C_p(T_3-T_2) = C_p.\left[T_3-\left(T_1+\left(\frac{T_{2s}-T_1}{\eta_C}\right)\right)\right] = C_p.\left[T_3-\left(T_1+\left(\frac{T_1.\, r_p^{\frac{(\gamma-1)}{\gamma}}-T_1}{\eta_C}\right)\right)\right] \tag{B.14}$$

The optimum actual efficiency of Brayton cycle is then calculated as;

$$\eta_{th,act,optimum} = \frac{W_{net}}{Q_{add}} = \frac{\eta_T.\, C_p\left(T_3 - \frac{T_3}{\sqrt{\frac{T_3}{T_1}\eta_T\eta_C}}\right) - \frac{C_p\left(T_1.\sqrt{\frac{T_3}{T_1}\eta_T\eta_C} - T_1\right)}{\eta_C}}{C_p.\left[T_3 - \left(T_1 + \left(\frac{T_1.\sqrt{\frac{T_3}{T_1}\eta_T\eta_C} - T_1}{\eta_C}\right)\right)\right]} \tag{B.15}$$

$$\eta_{th,act} = \frac{W_{net}}{Q_{add}} = \frac{\eta_T.\, T_3\left(1 - \frac{1}{\sqrt{\frac{T_3}{T_1}\eta_T\eta_C}}\right) - \frac{T_1}{\eta_C}\left(\sqrt{\frac{T_3}{T_1}\eta_T\eta_C} - 1\right)}{\left[T_3 - T_1\left(1 + \left(\frac{\sqrt{\frac{T_3}{T_1}\eta_T\eta_C} - 1}{\eta_C}\right)\right)\right]} \tag{B.16}$$

The actual Brayton efficiency is calculated as a function of top cycle temperature (T_{max}) and bottom cycle temperature (T_{min}).

$$\eta_{th,act} = \frac{\eta_T.\, T_{max}\left(1 - \frac{1}{\sqrt{\eta_T.\eta_C.\frac{T_{max}}{T_{min}}}}\right) - \frac{T_{min}}{\eta_C}\left(\sqrt{\eta_T.\,\eta_C.\,\frac{T_{max}}{T_{min}}} - 1\right)}{T_{max} - T_{min}.\left(1 + \frac{1}{\eta_C}.\left(\sqrt{\eta_T.\,\eta_C.\,\frac{T_{max}}{T_{min}}} - 1\right)\right)} \tag{B.17}$$

References

[1] Tlili Iskander, Timoumi Youssef, Nasrallah Sassi Ben. Analysis and design consideration of mean temperature differential Stirling engine for solar application. Renew Energy 2008;33:1911–21.

[2] Kongtragool Bancha, Wongwises Somchai. A review of solar-powered Stirling engines and low temperature differential Stirling engines. Renew Sustain Energy Rev 2003;7:131–54.

[3] Abbas Mohamed, Boumeddane Bousaad, Said Noureddine, Chikouche Ahmed. Dish Stirling technology: a 100 MW solar power plant using hydrogen for Algeria. Int J Hydrogen Energy 2011;36:4305–14.

[4] Ab Kadir MZA, Rafeeu Y, Adam NM. Prospective scenarios for the full solar energy development in Malaysia. Renew Sustain Energy Rev 2010;14:3023–31.

[5] Abbas M, Boumeddane B, Said N, Chikouche A. Techno-economic evaluation of solar Dish Stirling system for standalone electricity generation in Algeria. J Eng Appl Sci 2009;4:258–67.

[6] Andreas Poullikkas, George Kourtis, Ioannis Hadjipaschalis. Parametric analysis for the installation of solar dish technologies in Mediterranean regions. Renew Sustain Energy Rev 2010;14:2772–83.

[7] Klaib Helmut, Kohler Rainer, Nitsch Joachim, Sprengel Uwe. Solar thermal power plants for solar countries-technology, economics and market potential. Appl Energy 1995;52:165–83.

[8] Ahmadi Mohammad Hossien, Hosseinzade Hadi. Investigation of solar collector design parameters effect onto solar Stirling engine efficiency. J Appl Mech Eng 2012;1:1. http://dx.doi.org/10.4172/2168-9873.1000102.

[9] Koichi HIRATA. Development of a small 50W class stirling engine. < https://www.nmri.go.jp/eng/khirata/list/minieco/isme_50w.pdf > .

[10] Batmaz Ihsan, Ustün Süleyman. Design and manufacturing of a V-type Stirling engine with double heaters. Appl Energy 2008;85:1041–9.

[11] Cinar Can, Karabulut Halit. Manufacturing and testing of a gamma type Stirling engine. Renew Energy 2005;30:57–66.

[12] Shuang-Ying Wu, Xiao Lan, Cao Yiding, Li Y-Rong. A parabolic dish/AMTEC solar thermal power system and its performance evaluation. Appl Energy 2010;87:452–62.

[13] Rix DH. Some aspects of the outline design specification of a 0.5 kW Stirling engine for domestic scale co-generation. In: Proc instn mech engrs, vol. 210. A01594 @ IMechE; 1996.

[14] Solar Stirling Assessment. < http://www.engr.colostate.edu/~marchese/mech337-10/epri.pdf > .

[15] Gallup DR, Kesseli JB. A solarized Brayton engine based on turbo-charger technology and the DLR receiver. In: Proceedings of the IECEC, AIAA-94-3945-CP, Monterey, CA; 1994.

[16] Nizetic S, Klarin B. A simplified analytical approach for evaluation of the optimal ratio of pressure drop across the turbine in solar chimney power plants. Appl Energy 2010;87:587–91.

[17] Nafey AS, Sharaf MA, Garcia-Rodriguez Lourdes. A new visual library for design and simulation of solar desalination systems (SDS). Desalination 2010;259:197–207.

[18] Sharaf Eldean Mohamed A, Soliman AM. A new visual library for modeling and simulation of renewable energy desalination systems (REDS). Desalinat Water Treatm 2013:1–16. http://dx.doi.org/10.1080/19443994.2013.777369.

[19] Siva Reddy V, Kaushik SC, Tyagi SK. Exergetic analysis and performance evaluation of parabolic dish Stirling engine solar power plant. Int J Energy Res 2013;37:1287–301. http://dx.doi.org/10.1002/er.2926.

[20] Hafez AZ, Soliman Ahmed, El-Metwally KA, Ismail IM. Solar parabolic dish Stirling engine system design, simulation, and thermal analysis. Energy Convers Manage 2016;126:60–75.

[21] Nag PK. Basic and applied thermodynamics. New Delhi: Tata McGraw-Hill0-07-047338-2; 2002.

[22] Al-Dafaie Ameer Mohammed Abbas, Dahdolan Mohame-Eslam, Al-Nimr Mohamed A. Utilizing the heat rejected from a solar dish Stirling engine in potable water production. Sol Energy 2016;136:317–26.

[23] Duffie JA, Beckman WA. Solar engineering of thermal processes. Hoboken (New Jersey): John Wiley & Sons Inc; 2013.

[24] Fraser Paul R. Stirling dish system performance prediction model [M.Sc. Thesis]. UNIVERSITY OF WISCONSIN-MADISON; 2008.

[25] http://www.periodictable.com/Elements/036/data.html.

[26] http://webbook.nist.gov/.

[27] Sharaf Eldean Mohamed A, Soliman AM. A novel study of using oil refinery plants waste gases for thermal desalination and electric power generation: energy, exergy & cost evaluations. Appl Energy 2017;195:453–77.

[28] Çengel Yunus A, Boles Michael A. Thermodynamics: an engineering approach. 8th ed. McGraw-Hill Education; 2014. ISBN-10: 0073398179.

[29] Lovegrove K, Stein W. Concentrating solar power technology: principles, developments and applications. Elsevier; 19th October 2012. Hardcover ISBN: 9781845697693.

[30] Greenwood NN, Earnshaw A. Chemistry of the elements. 2nd ed. Oxford: Butterworth-Heinemann; 1997. ISBN 0-7506-3365-4.